Improved assessment of aerosol absorption using OMI-MODIS joint retrieval

S. K. Satheesh,[1,2] O. Torres,[3] L. A. Remer,[2] S. Suresh Babu,[4] V. Vinoj,[1] T. F. Eck,[2] R. G. Kleidman,[2] and B. N. Holben[2]

Received 23 August 2008; revised 12 November 2008; accepted 11 December 2008; published 13 March 2009.

[1] The Ozone Monitoring Instrument (OMI) aboard EOS-Aura and the Moderate Resolution Imaging Spectroradiometer (MODIS) onboard EOS-Aqua fly in formation as part of the A-train. Though OMI retrieves aerosol optical depth (AOD) and aerosol absorption, it must assume aerosol layer height. The MODIS cannot retrieve aerosol absorption, but MODIS aerosol retrieval is not sensitive to aerosol layer height and with its smaller pixel size is less affected by subpixel clouds. Here we demonstrate an approach that uses MODIS-retrieved AOD to constrain the OMI retrieval, freeing OMI from making an a priori estimate of aerosol height and allowing a more direct retrieval of aerosol absorption. To predict near-UV optical depths using MODIS data we rely on the spectral curvature of the MODIS-retrieved visible and near-IR spectral AODs. Application of an OMI-MODIS joint retrieval over the north tropical Atlantic shows good agreement between OMI and MODIS-predicted AODs in the UV, which implies that the aerosol height assumed in the OMI-standard algorithm is probably correct. In contrast, over the Arabian Sea, MODIS-predicted AOD deviated from the OMI-standard retrieval, but combined OMI-MODIS retrievals substantially improved information on aerosol layer height (on the basis of validation against airborne lidar measurements). This implies an improvement in the aerosol absorption retrieval, but lack of UV absorption measurements prevents a true validation. Our study demonstrates the potential of multisatellite analysis of A-train data to improve the accuracy of retrieved aerosol products and suggests that a combined OMI-MODIS-CALIPSO retrieval has large potential to further improve assessments of aerosol absorption.

Citation: Satheesh, S. K., O. Torres, L. A. Remer, S. S. Babu, V. Vinoj, T. F. Eck, R. G. Kleidman, and B. N. Holben (2009), Improved assessment of aerosol absorption using OMI-MODIS joint retrieval, *J. Geophys. Res.*, *114*, D05209, doi:10.1029/2008JD011024.

1. Introduction

[2] The Earth's climate is strongly influenced by the manner in which solar radiation is absorbed and reflected in the atmosphere [*Kaufman et al.*, 2002; *Andreae et al.*, 2005; *Seinfeld*, 2008]. In recent years, there has been a substantial increase in interest in the influence of natural and anthropogenic aerosols on the climate through both direct and indirect radiative effects [*Satheesh and Moorthy*, 2005]. Several extensive investigations and coordinated field campaigns have been carried out to assess the impact of aerosols on climate [*Kaufman et al.*, 1998; *Bates*, 1999; *Russell and Heintzenberg*, 2000; *Seinfeld et al.*, 2004]. Field experiments, however, provide data only for a small region and/or time period, and therefore, estimates of global aerosol effects must rely on a combination of model results, constrained by a variety of observations including satellite remote sensing to provide a global view of the aerosol system.

[3] The effect that aerosols impose on the climate system depends on the radiative or optical properties of the particles, as well as on the total aerosol loading. The degree to which these particles absorb light, is a key parameter needed to quantify aerosol radiative effects and estimate aerosol forcing on the climate system. A moderate change in absorption properties can change the sign of the aerosol radiative forcing from negative (cooling) to positive (warming) [*Hansen et al.*, 1997; *Kaufman et al.*, 2001].

[4] Presently aerosol absorption is poorly quantified because aerosols vary widely depending on their composition and origin. Aerosols as varied as carbonaceous particles and desert dust can both absorb light. Adding to the complexity, there exists no direct relationship between aerosol mass, optical depth and the particles' radiative impacts [*Seinfeld*

[1]Centre for Atmospheric and Oceanic Sciences, Indian Institute of Science, Bangalore, India.
[2]Laboratory for Atmospheres, NASA Goddard Space Flight Center, Greenbelt, Maryland, USA.
[3]Department of Atmospheric and Planetary Sciences, Hampton University, Hampton, Virginia, USA.
[4]Space Physics Laboratory, Vikram Sarabhai Space Centre, Thiruvananthapuram, India.

Copyright 2009 by the American Geophysical Union.
0148-0227/09/2008JD011024

and Pandis, 1998]. The radiative effects of carbonaceous aerosol vary depending on the production mechanism such as forest fires, manmade burning or transport. Similarly, radiative effects of dust aerosol also vary depending on the region of origin and possible contamination while being transported to other regions by atmospheric circulation processes. Carbonaceous aerosols have significant roles in climate modification because of their high absorption characteristics. A brief review of both in situ and laboratory techniques to measure aerosol absorption has been provided in *Torres et al.* [2005] and a detailed description is available elsewhere [*Horvath*, 1993; *Heintzenberg et al.*, 1997; *Weingartner et al.*, 2003; *Arnott et al.*, 2005]. Even though laboratory analysis can provide aerosol absorption on a localized manner (or at most on a regional basis), satellite remote sensing stands a better option (even with the inherent limitations) in a global scenario.

[5] Retrieval of aerosol absorption using satellite remote sensing is an important but difficult problem [*Kaufman et al.*, 2001]. The relative importance of scattering and absorption in satellite remote sensing has been addressed by various investigators since the 1980s [*Fraser and Kaufman*, 1985; *Kaufman et al.*, 2001]. However, few satellite sensors currently make operational retrievals of aerosol absorption, and none of these retrievals are validated. The Multiangle Imaging Spectro-Radiometer (MISR) provides a measure of absorption along with its retrieval of aerosol particle properties [*Diner et al.*, 1998, 2002]. The Moderate Resolution Imaging Spectroradiometer (MODIS) is now providing a measure of aerosol absorption over bright land surfaces as part of its new Deep Blue algorithm [*Hsu et al.*, 2004]. Also, the Ozone Monitoring Instrument (OMI) provides a retrieval of aerosol absorption with its aerosol product [*Levelt et al.*, 2006; *Schoeberl et al.*, 2006; *Torres et al.*, 2007]. Still retrieving aerosol absorption from satellite remote sensing remains a challenge, especially when using a single sensor. Hence, multisensor retrievals become increasingly relevant when observations are automatically near-collocated in time and in space as it is the case with A-train sensors [*Anderson et al.*, 2005]. In this paper, we make an effort to improve the assessments of aerosol absorption using multiple satellite data, a combination of OMI and MODIS.

2. MODIS and OMI Aerosol Retrievals

[6] Both MODIS and OMI produce operational aerosol products, but use entirely different methods that leverage the strengths of each individual sensor. MODIS has 36 channels spanning the spectral range from 410 to 14400 nm representing three spatial resolutions: 250 m (2 channels), 500 m (5 channels), and 1 km (29 channels). The aerosol retrievals make use of eight of these channels (410–2130 nm) to retrieve aerosol characteristics [*Hsu et al.*, 2004; *Remer et al.*, 2005]. The MODIS aerosol algorithm consists of three independent algorithms, two derive aerosol characteristics over land and the other over ocean. It is the ocean algorithm and the ocean aerosol products that we will use in combination with OMI in this paper.

[7] The ocean algorithm makes use of its fine spatial resolution observations and wide spectral range to mask out suspended river sediments, clouds and sunglint, then inverts the radiance at 6 wavelengths (550 to 2130 nm) to retrieve spectral aerosol optical depth (AOD) and particle size information [*Tanré et al.*, 1996, 1997]. Because the water leaving radiance is essentially zero at 0.87 μm, once suspended sediments are identified and masked, the primary optical depth retrieval is heavily weighted to this channel. The other five channels provide information on the spectral properties of the aerosol, and from there particle size is retrieved. The broad spectral range from 0.55 μm to 2.13 μm provides sufficient information to retrieve the accurate spectral signature of the aerosol. The MODIS ocean aerosol retrieval is documented fully in the literature and will not be reiterated here [*Tanré et al.*, 1997; *Levy et al.*, 2003; *Remer et al.*, 2005].

[8] The OMI near-UV aerosol algorithm (OMAERUV) uses measurements made at two wavelengths in the UV region (354 and 388 nm) to take advantage of the large sensitivity of the upwelling radiances to aerosol absorption in this spectral region [*Torres et al.*, 1998]. The OMAERUV aerosol products are UV Aerosol Index, and aerosol extinction and absorption optical depths at 388 nm.

[9] Aerosol extinction optical depth (AOD) and aerosol absorption optical depth (AAOD) at 388 nm are derived using a standard inversion algorithm that uses precomputed reflectances for a set of assumed aerosol models. Three major aerosol types are considered: desert dust, carbonaceous aerosols associated with biomass burning, and weakly absorbing sulfate-based aerosols. Each aerosol type is represented by seven aerosol models of varying single-scattering albedo, for a total of twenty-one microphysical models. Since the retrieval algorithm is sensitive to the aerosol height [*Torres et al.*, 2005], results are reported for five different assumptions on the location of the aerosol center of mass: at the surface, and at 1.5, 3.0, 6.0 and 10.0 km above the surface. In addition, best estimate values of AOD and AAOD associated with a particular choice of aerosol vertical distribution are made available.

[10] Given the large size (13 $\times$ 24 km at nadir) of the OMI pixels subpixel cloud contamination is a prevailing problem resulting in the overestimation of the extinction optical depth and underestimation of the single-scattering coalbedo [*Torres et al.*, 1998]. However, in the calculation of the absorption optical depth a cancellation of errors takes place that allows the AAOD retrieval even in the presence of small amounts of cloud contamination. For a detailed description of the algorithm the reader is referred to the overview paper by *Torres et al.* [2007].

3. Why OMI-MODIS Joint Retrieval?

[11] The Aura-OMI and the Aqua-MODIS instruments fly on A-train platforms within 8 min of each other. The quasi-simultaneity of their observations makes these sensors suitable for the application of a combined retrieval approach. OMI retrieves both aerosol extinction optical depth (AOD) and absorption information reported as single-scattering albedo, while MODIS retrieves AOD and particle size [*Remer et al.*, 2005; *Torres et al.*, 2007]. The OMI retrieved information on absorbing aerosols depends on the assumed aerosol layer height. The MODIS retrieval algorithm, on the other hand, is insensitive to the aerosol vertical distribution but it needs to assume a value of the single-scattering albedo. OMI pixels at a spatial resolution of 13 km by 24 km are often

cloud contaminated (owing to large pixel size) whereas MODIS pixels at a resolution of 500 m are significantly less affected by cloud contamination. Thus a combination of the observations from these two sensors offers the opportunity of taking advantage of their individual strengths: OMI's unique sensitivity to aerosol absorption and MODIS accurate retrievals of aerosol optical depth and information on aerosol particle size.

[12] Combining the information from the two sensors is not as straightforward as simply joining the spectral radiance observations of OMI and MODIS into a single "super" instrument. Performing a joint inversion on a joined OMI-MODIS spectrum of radiances requires careful intercalibration of the two sensors and adjusting for different view geometries and the time difference. Significant uncertainties can be introduced into the retrieval if these adjustments are not done perfectly. However, if we instead pass information from one instrument to the other, after the initial retrieval has been made, problems associated with geometry and calibration issues are significantly reduced. In this approach it is assumed that the retrieval algorithm of each individual sensor has already been optimized to produce the most accurate product given the input radiances measured by that particular sensor.

[13] MODIS's strength is the availability of several channels in the Visible through Short Wave Infrared (SWIR) bands that permit accurate retrieval of AOD across a wide spectral range, especially over ocean. OMI's strength is its sensitivity to aerosol absorption in the near-UV. However, the accuracy of OMI's retrieval is limited by the fact that the standard aerosol algorithm is sensitive to assumptions of aerosol height. The approach used in this work consists on using the MODIS retrieved AOD as input to the OMI retrieval. By doing so the OMI algorithm can then makes use of the two pieces of information available to infer both the aerosol layer height and the aerosol single-scattering albedo. A difficulty in this method is the need to extrapolate the MODIS retrieved AOD to the near-UV (388 nm) where OMI requires the AOD information for its retrieval. The extrapolation method may work quite well when the aerosol type is predominantly made up of large particles and, therefore, the optical depth is only weakly wavelength-dependent as it is the case with desert dust aerosols. However, for small particles as in the case of carbonaceous and pollution aerosols, the accurate extrapolation is a challenging procedure. Thus, the first step toward this approach is to examine whether MODIS can predict near-UV optical depths with sufficient accuracy to be used as input in the OMI inversion scheme.

4. Can MODIS Visible and Near-IR Observations Predict Near-UV Optical Depths?

[14] We can test MODIS' ability to estimate AOD in the UV, by comparing the estimated UV AOD with high-quality ground-based observations. The Aerosol Robotics Network (AERONET) instruments observe aerosol optical depths at seven spectral channels (0.34, 0.38, 0.44, 0.50, 0.66, 0.87 and 1.020 μm) and retrieve total column precipitable water vapor using the 0.94 μm channel. Under cloud-free conditions, the uncertainty in calculation of AOD is $< \pm 0.01$ for wavelengths >440 nm and $< \pm 0.02$ for shorter wavelengths [*Holben et al.*, 1998; *Eck et al.*, 1999]. We use a data set of MODIS-AERONET collocations where each MODIS AOD value represents the spatial mean AOD from a box of 25 retrievals centered on the AERONET station, and the AERONET AOD represents the temporal mean of AERONET observations taken ±30 min of MODIS overpass [*Ichoku et al.*, 2002].

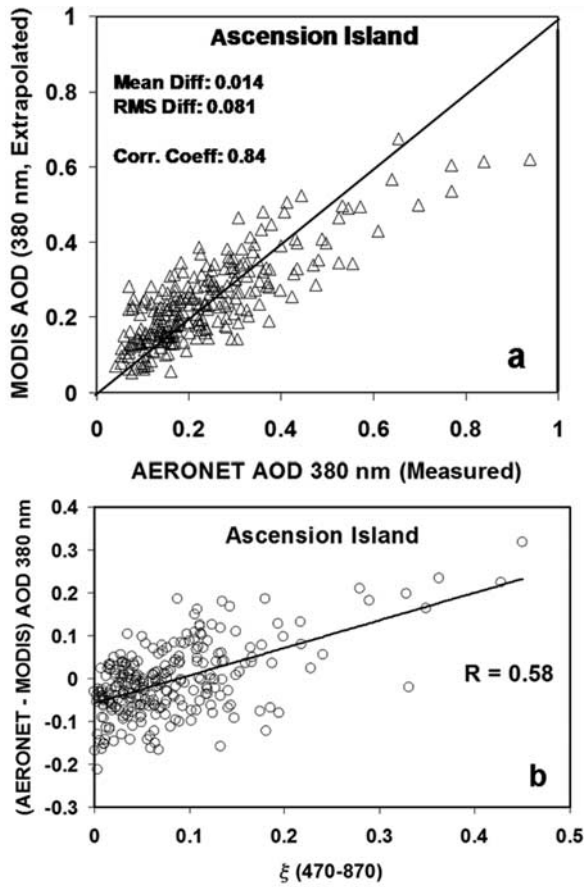

Figure 1. (a) Comparison of Moderate Resolution Imaging Spectroradiometer (MODIS) (extrapolated) AODs at 380 nm with those measured by AERONET at Ascension Island. (b) Difference between (extrapolated) and AERONET AODs plotted against curvature of the MODIS spectral AODs.

[15] We apply a linear least square fitting (in a log-log scale) to the MODIS observations of AOD at 0.47, 0.55, 0.66, and 0.87 μm, and use this fit to extrapolate the MODIS value to 0.38 μm. Figure 1a shows UV AOD (τ_{aM} at 0.38 μm) linearly extrapolated (in a log-log scale) using MODIS visible channels compared with those measured by the AERONET Sun photometer (τ_{aA}) at Ascension island (7S, 14W). The extrapolation shows reasonably good agreement with AERONET with deviations less than 0.1 at low AODs (<0.4 at UV wavelengths). However, we see substantial differences, as high as ~0.3, at larger AOD.

[16] The major challenge in this exercise is the contrasting influence of various aerosol species to UV, visible and near-IR wavelengths. For example, super-micron-sized (coarse mode) sea salt and dust particles influence near-IR wavelengths similar to the visible, thereby flattening the

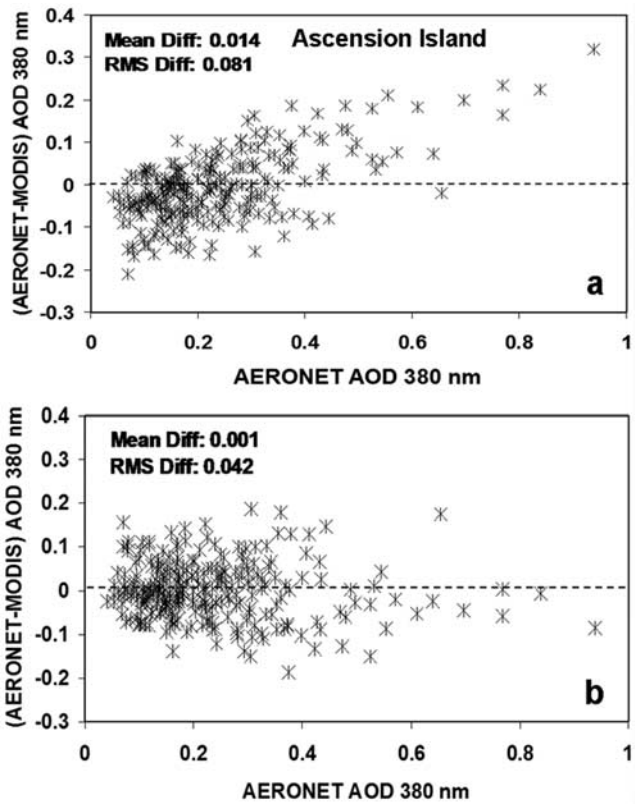

Figure 2. Difference between (extrapolated) and AERONET AODs plotted against AERONET AOD at 380 nm in the case of Ascension Island (a) before correction and (b) after correction. The RMS difference is reduced to half after correction.

spectral AOD signature. In fact a completely coarse mode dominated aerosol has negligible spectral AOD variation. On the other hand, fine mode sulphate and biomass burning aerosols influence the shorter wavelengths more, steepening the spectral slope. When viewed in this perspective, one common reason for the deviations of τ_{aM} from τ_{aA} [hereafter referred as $\Delta\tau$ (380 nm)] could be the sea salt and (or) dust influence at near-IR AODs, which weakens spectral dependence and hence predictability of UV AODs using MODIS visible channels. Analysis of numerous AOD spectra of many global aerosol types from AERONET data has shown that the departure from linearity of AOD versus wavelength in log-log space occurs when fine mode aerosol is dominant and especially when fine mode aerosol size increases, typically due to aging (coagulation) or hygroscopic growth [*Eck et al.*, 1999]. Dominance of fine aerosols to which UV wavelengths are more sensitive compared to visible and near-IR is the primary reason for differences in MODIS-predicted and AERONET-measured UV AODs.

[17] We find that we can improve the linear extrapolation into the UV by including information on the AOD spectral curvature. In essence this corrects for the variable sensitivity of the aerosol species to different ranges of the spectra as discussed above. We define ξ (470–870), as the arithmetic difference between AOD at 470 and 870 nm, and show the dependence of $\Delta\tau$ (0.38 μm) on ξ in Figure 1b at Ascension Island. A statistically significant correlation coefficient (ρ) of 0.58 was observed between $\Delta\tau$ (0.38 μm) versus ξ. This exercise [over Ascension Island (7S, 14W)] yielded an empirical equation of the form,

$$\Delta\tau_{0.38} = 0.64\xi - 0.057 \quad (1)$$

[18] The applicability of equation (1) for correcting the τ_{aM} is evident from Figures 2a and 2b where RMS difference reduced to half of what was achieved before the curvature correction. A similar exercise at Male Island (4N, 73E) in the Indian Ocean yielded similar results (Figures 3a and 3b), where the regression equation was calculated as

$$\Delta\tau_{0.38} = 0.69\xi - 0.048 \quad (2)$$

[19] A substantial reduction of root mean square (RMS) difference was also observed in Male when corrected using the empirical relation (equation (2)). We applied this approach at several other island sites [Midway Island (28N, 177W), Azores (38N, 28W), Coconut Island (21N,157W), Nauru (0S, 166E), and Tahiti (17S, 149W)] (see Figure 4a). An average picture of the correction/adjustment factor, $\Delta\tau_{0.38}$, emerged from the analysis. Figure 4b shows the range of empirical regression equations by the shaded region, while the vertical bars are standard deviations about the mean line. This leads to an equation (which is an average of all sites considered) of the form:

$$\Delta\tau_{0.38} = 0.54\xi - 0.041 \quad (3)$$

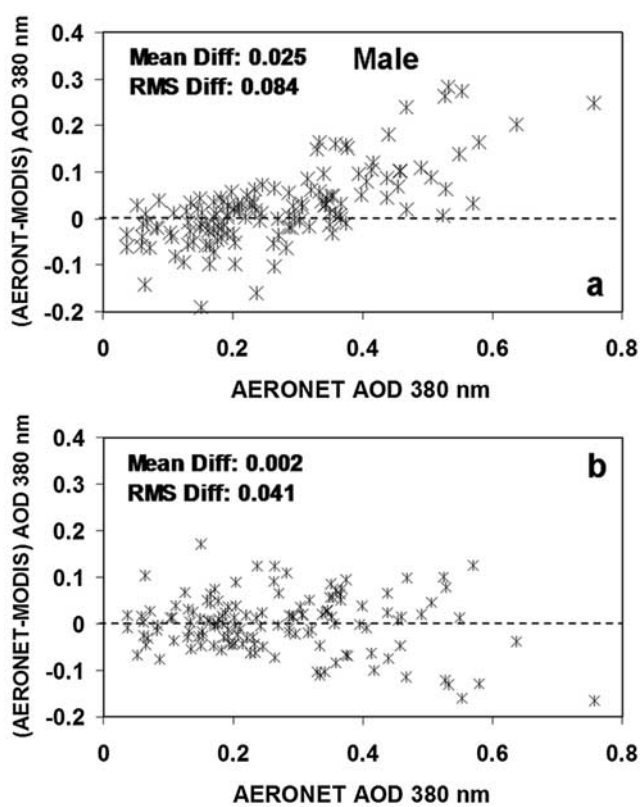

Figure 3. Same as Figure 2, but for Male Island in the Indian Ocean.

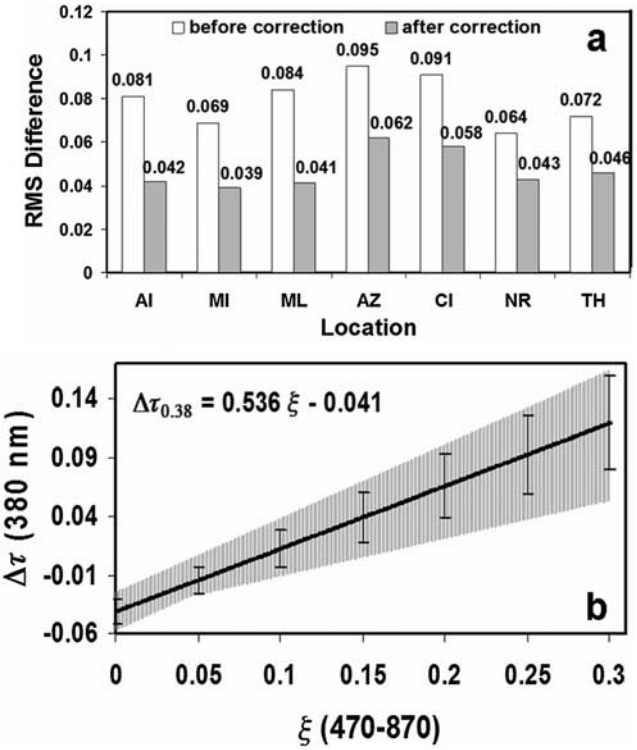

Figure 4. (a) The RMS differences before and after correction estimated for several island sites. Here AI, MI, ML, AZ, CI, NR, and TH represent Ascension Island, Midway Island, Male, Azores, Coconut Island, Nauru, and Tahiti, respectively. (b) The spread of correction ($\Delta\tau_{0.38}$) as a function of curvature of spectral AODs using all sites considered where shaded region represent the range of values and vertical bars are standard deviations about the mean line.

[20] Figure 4a shows the substantial reduction of RMS difference observed when the linear extrapolations were corrected using equation (3).

[21] Does this mean that equation (3) is universally applicable? There may be cases where it cannot be used. *Kirchstetter et al.* [2004] have reported that presence of organic carbon can cause strong spectral dependence in absorption in UV wavelengths while having no signature in visible wavelengths. In such circumstances, it is difficult to predict UV optical depths using MODIS (visible and near-IR) data. Additionally for desert dust dominated aerosol, there should be minimal spectral curvature of AOD even at high levels of AOD.

5. Hybrid Approach: OMI-MODIS Joint Retrieval

[22] Now that we have established that MODIS can, under most circumstances, predict UV (0.38 μm) optical depths (hereafter referred as MODIS-predicted AODs), we can follow a hybrid approach involving OMI and MODIS data in which MODIS can constrain the OMI retrieval by providing the AOD at 0.38 μm. An added benefit of this approach is to improve OMI cloud screening. The relatively large pixel size of OMI (13 km $\times$ 24 km) compared to sensors such as MODIS, results in larger levels of subpixel cloud contamination in the OMI pixels. When an OMI pixel is cloud contaminated, the retrieval algorithm overestimates extinction optical depths and underestimates absorption optical depths [*Torres et al.*, 2007]. By collocating OMI and MODIS pixels, it is possible to indirectly apply MODIS cloud screening to OMI data. In this way collocated OMI pixels, which have a MODIS counter part will have much reduced cloud contamination.

[23] Several ordered pairs of AOD and absorption AOD (AAOD) are reported in the standard OMI product for different assumptions of aerosol layer height including the surface and 1.5, 3.0, 6.0 and 10 km above surface. The OMI product also indicates the best estimate of AOD and AAOD based on the climatology of layer heights at different geographic regions [*Torres et al.*, 2007]. A transport-model-generated [*Chin et al.*, 2000] climatological database of aerosol layer heights is currently used in the OMI algorithm to prescribe the height of desert dust aerosols. For carbonaceous aerosols an altitude of either 3 or 6 km is assumed depending on latitude [*Torres et al.*, 2007]. Thus, the assumed values of aerosol layer height are used to constrain the other two free parameters of the retrieval, AOD and AAOD. However, any one of the three free parameters, if known, could be used to constrain the retrieval of the other two. If total AOD were known, then we could choose height and AAOD with greater certainty.

[24] The success of using the MODIS visible and near-IR spectral AODs to estimate UV optical depth suggests that we can use MODIS-predicted AOD in the UV to constrain the OMI inversion, and leave OMI free to return information on aerosol height and most importantly, aerosol absorption. Readers may note that in the case of sulphate aerosol, retrieved AOD in OMI-standard retrieval is independent of altitude and hence this approach is not applicable. In the discussion that follows we will use the term "MODIS-predicted AOD" to refer to the near-UV optical depth obtained by extrapolation of the visible and near-IR MODIS observations. The OMI retrieved values of single-scattering albedo and aerosol layer heights using the MODIS-predicted AOD are referred to as OMI-MODIS retrievals as opposed to the standard values produced by the OMI standard algorithm. Also, the terms "MODIS-adjusted retrieval" and "OMI-MODIS joint retrieval" are used interchangeably to represent retrievals of aerosol layer height and single-scattering albedo. Evaluation of the uncertainties shows that for an uncertainty in the extrapolated UV AOD of ±0.05, uncertainty in aerosol layer height is ±0.23 km and that in SSA is ±0.017.

[25] We test a joint OMI-MODIS retrieval in three regions (marked in Figure 5): East Tropical N. Atlantic (10–30N, 20–30W), Central Tropical N. Atlantic (10–30N, 30–40W) and Arabian Sea (10–20N, 60–70E). In each region we collocated OMI and MODIS retrievals, used the MODIS-retrieved spectral AOD in the visible and near-infrared to estimate AOD at 0.38 μm and then used that value in the standard OMI retrieval to fix the aerosol layer height and AAOD. The layer height and AAOD are interpolated from the five possible values listed in the retrieval. Single-scattering albedo (ω_0) values are estimated as (AOD-AAOD)/AOD. Only OMI data with Quality Flag = 0, least cloud affected, were used in the analysis. We analyzed data during the entire year of 2006.

Figure 5. Map showing the two tropical north Atlantic study regions and the Arabian Sea study region.

[26] The major observations from the Atlantic are shown in Figure 6.

[27] 1. On an average MODIS-predicted and OMI-standard retrievals of AOD (0.38 μm), agree within ±0.1. OMI-MODIS retrievals of single-scattering albedo (ω_0) and aerosol layer height (H) agreed with OMI-standard values (on an average) to within ±0.02 and ±1km, respectively.

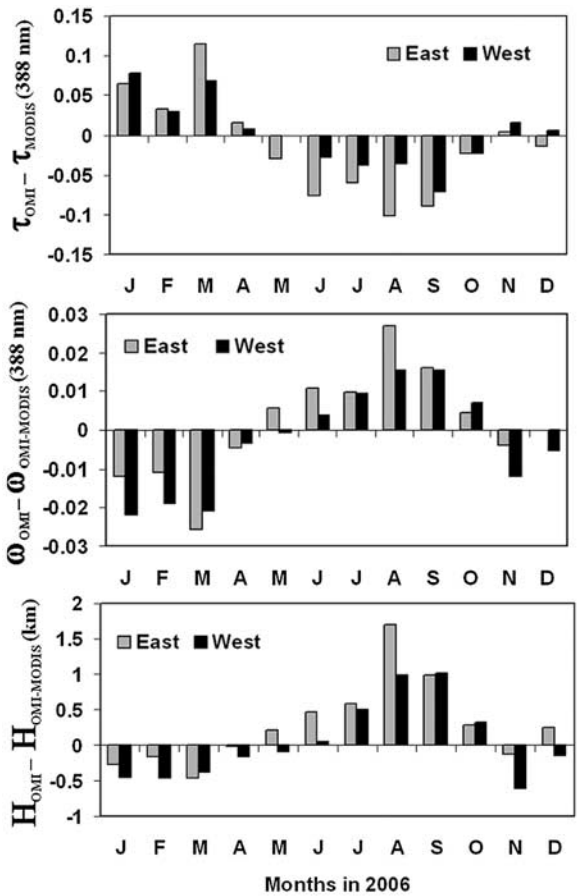

Figure 6. The difference between OMI retrieval and OMI-MODIS combined retrievals. Aerosol optical depth, single-scattering albedo, and layer height are shown as three panels for the North Atlantic. East and west represents the east box and west box considered over the North Atlantic.

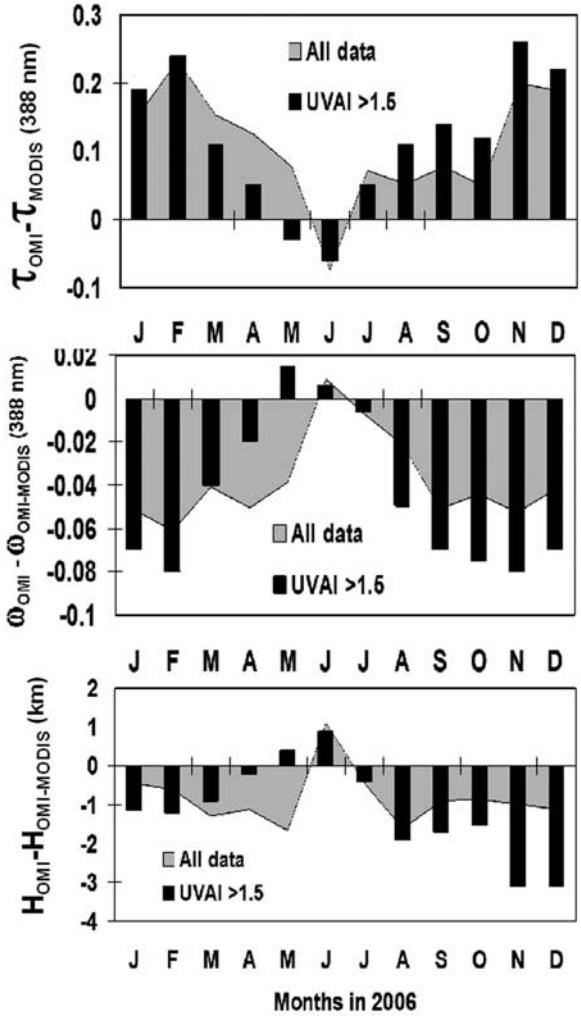

Figure 7. The difference between OMI retrieval and OMI-MODIS combined retrievals. Aerosol optical depth, single-scattering albedo, and layer height are shown as three panels for the Arabian Sea. Two cases are shown. In the first case, all data were used, whereas in second case, data corresponding to UVAI >1.5 only were used.

[28] 2. During January to April, OMI-standard AOD values are larger than the MODIS-predicted values. OMI-standard values of single-scattering coalbedo are lower than their OMI-MODIS counterparts. During the rest of the year it was the reverse situation.

[29] 3. In general, the agreement between MODIS-predicted and OMI-standard optical depths (τ_a) (and consequently between OMI-standard and OMI-MODIS retrievals of ω_0 and H), was better in the West Atlantic as compared to the East Atlantic (Figure 6).

[30] Over the North Atlantic, the general agreement between MODIS-predicted and OMI-standard values of AOD implies that the aerosol height (and size distribution) assumed in the OMI algorithm is probably correct for this area.

[31] Over the Arabian Sea (Figure 7), differences as large as 0.26 were observed between the MODIS-predicted and OMI-standard τ_a values, whereas the observed differences between OMI-MODIS and OMI-standard values of ω_0 and H were as large as 0.08 and 3.2 km respectively. Differences

between OMI-MODIS and OMI-standard retrievals can be due either to an incorrect assumption of aerosol height or to an incorrect assumption of aerosol type, particularly whether fine or coarse particles. We checked the OMI-standard assumption of aerosol type against MODIS retrievals of particle size for 2 months, April and November. The OMI-standard assumption disagreed with the MODIS retrieval 21% of the time in April and 32% of the time in November. Because the majority of cases appear to use the correct assumption of aerosol type, it may be worthwhile to revisit the OMI assumption of aerosol height in this region. Still, we note that in the future we could further improve the OMI-standard retrieval by passing information from MODIS on particle size as well as AOD, and thus further constrain the assumptions in the OMI retrieval.

[32] Another product of the standard OMI aerosol retrieval is the UV aerosol index (UVAI), which is an indicator of UV absorbing aerosols [see *Torres et al.*, 2007 for a description of UVAI]. We can use UVAI to further explore the reasons why the standard OMI retrieval some times does not match with the MODIS-predicted estimate. Since UVAI is sensitive to UV absorbing aerosols, it is used in OMI retrievals to differentiate UV absorbing aerosols from nonabsorbing aerosol types. The OMI inversion uses precomputed lookup tables for a set of assumed aerosol models. Major aerosol types considered in the OMI retrieval are (1) desert dust, (2) carbonaceous aerosol, and (3) sulphate aerosols. Keeping this in mind, we have examined the variation of mean differences between MODIS-predicted and OMI-standard τ_a values, and between OMI-MODIS and OMI-standard values of ω_0 and H as a function of UVAI. Over the North Atlantic, it appears that the higher the UVAI, the better the agreement between the standard OMI retrieval and MODIS-predicted AOD and therefore the standard and adjusted OMI results are very close. The resulting good agreement suggests that the aerosol type is consistently identified as dust by the two algorithms and that the OMI prescribed aerosol layer height closely represents the actual situation. Note that dust also has near-neutral spectral dependence in AOD. However, over the Arabian Sea the differences only increase as UVAI increases (Figure 7). Here agreement is far better at low UVAI.

6. How Representative is the OMI-MODIS Joint Retrieval?

[33] Results discussed in the previous sections suggest that by combining OMI and MODIS data, we can substantially improve information on aerosol layer height and hence aerosol absorption. To validate these joint retrievals, we need measurements of aerosol vertical distribution as well as aerosol single-scattering albedo. Data on aerosol vertical profiles are available (though sparse) whereas direct measurements of UV aerosol single-scattering albedo or other absorption parameters in the total column have not been available except in very isolated situations. Therefore, we cannot validate the over ocean retrievals of aerosol absorption, but we do make an effort to validate aerosol layer height retrievals.

[34] During March–May 2006, airborne lidar measurements were made over the Arabian Sea and Bay of Bengal regions using an instrumented aircraft (Beachcraft 200) of the National Remote Sensing Agency [*Moorthy et al.*, 2008 for details] in India. The micro pulse lidar (model MPL1000 of Science and Engineering Services Inc., USA) was used for profiling aerosol extinction [see *Satheesh et al.*, 2006a, for details]. These airborne lidar measurements were carried out as part of Integrated Campaign for Aerosols, gases and Radiation Budget (ICARB) sponsored by Indian Space Research Organisation's Geosphere Biosphere Programme (ISRO-GBP) [*Moorthy et al.*, 2008].

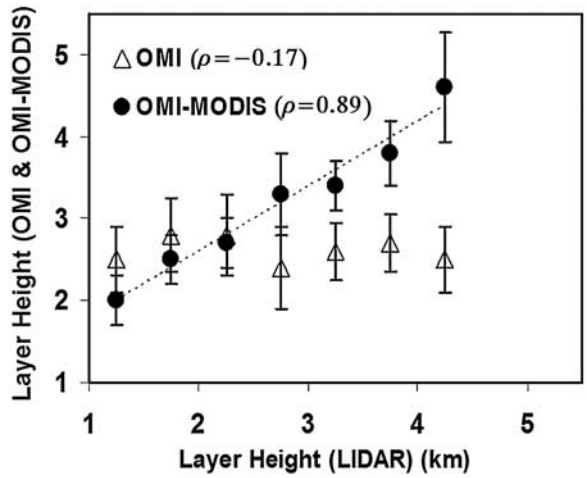

Figure 8. Comparison of aerosol layer height obtained from OMI retrieval and OMI-MODIS combined retrievals with those obtained from airborne lidar.

[35] The aerosol profiles from airborne lidar show that aerosol extinction coefficient increases with height, reaches a maximum and then decreases. Aerosol layer heights are estimated by differentiating the extinction coefficient with respect to altitude and layer height is defined as height at which the derivative changes sign from positive to negative. A comparison of aerosol layer height from airborne lidar versus those obtained from OMI-MODIS joint retrievals (solid spheres) as well as OMI-standard retrievals (open triangles) is shown in Figure 8. An excellent correlation (ρ = 0.89) between lidar versus OMI-MODIS retrievals of layer heights was observed whereas correlation was poor in the case of the original OMI retrievals.

[36] The poor agreement between OMI-standard reporting of aerosol height and the lidar observations could either be due to poor assumptions of aerosol height in the retrieval or poor assumptions of aerosol type. We found that the OMI assumption of aerosol type agreed with the MODIS retrieval of particle size in 89% of the collocations. This is better than the 79% over the full month of April. Thus, part of the good agreement between OMI-MODIS retrieved height and the lidar observations are because the OMI assumptions of height were wrong, but aerosol type were correct. Agreement may not be as good for the full data period when both assumptions will be wrong more often. However, we note that in the future, supplying the OMI retrieval with particle size information from MODIS can further reduce uncertainties in the joint retrieval.

7. UV Single-Scattering Albedo and Aerosol Layer Height: Seasonal Trends

[37] The aerosol layer height and single-scattering albedo (at 388 nm) obtained for the three locations considered in

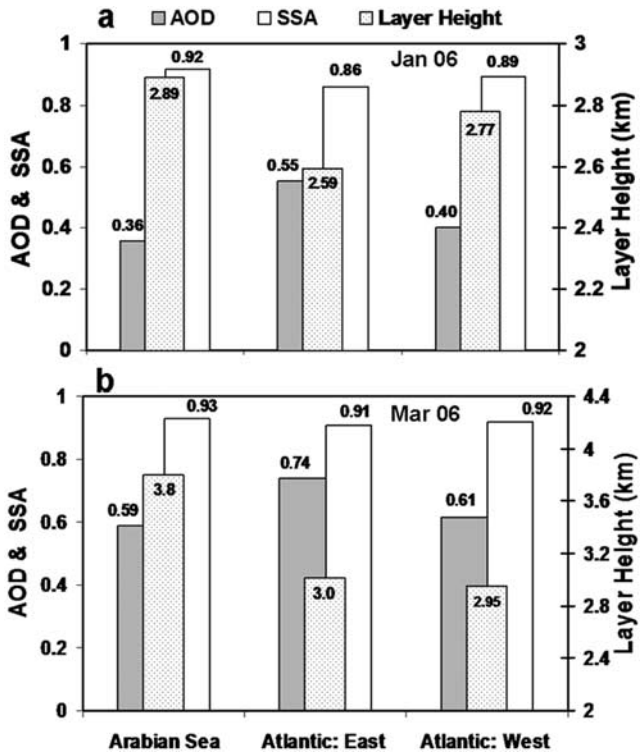

Figure 9. Aerosol layer height and single-scattering albedo (at 388 nm) obtained for the three locations considered in this study (North Atlantic and Arabian Sea) are shown for January and March for illustration.

this study (North Atlantic and Arabian Sea) are given in Table 1. Figure 9 shows the values for January and March 2006.

[38] The north Atlantic in the latitude band 10°N to 30°N receives transported aerosols from the African continent. These consist of desert dust from the Sahara, and also smoke from biomass burning in the Sahel and coastal West Africa. The dust is present all year, as it comes from various desert sources, but its peak intensity over the North Atlantic is during June and July. The biomass burning season occurs January through March or April, and while much of the smoke is transported to the south and across the Atlantic in a more southerly route than 10°N, some smoke does mix with the dust in our regions of interest.

[39] The Arabian Sea region, because of its particular geographical location, has a unique weather pattern attributed to the Indian monsoon and the associated winds that reverse direction seasonally. Most of the Arabian Sea is influenced by two contrasting air masses associated with the Asian monsoon system [*Asnani*, 1993; *Ramanathan et al.*, 2001]. During the winter monsoon (November to March), the winds over the Arabian Sea are mainly weak, northeasterly or northerly (from India). This implies that during the winter monsoon, winds carry aerosols from the Indian subcontinent to adjacent oceanic regions [*Satheesh et al.*, 1999]. From March onward, winds shift in direction from northeast to northwest. By April, the winds become northwesterly and westerly (from west Asia) and this continues until October.

[40] We see from the results in Table 1 that there is a systematic difference in the absorption properties of the aerosol as it moves westward from the African continent, becoming less absorbing (having a higher SSA) the further west it is observed. The annual mean difference in SSA is 0.02. At the same time, the retrieval suggests that the mean height of the transported aerosol layer has decreased roughly 300 m.

[41] Measurements of SSA in the UV are sparse and hence seasonal trends can be assessed only by logical reasoning. On the other hand, there have been some studies reporting on SSA in the visible wavelengths in these two regions. *Kaufman et al.* [2001], using remote sensing, inferred SSA (at 550 nm) of Saharan dust as 0.97 at 0.55 mm. Previous studies had estimated SSA for Saharan dust as low as 0.85 in the midvisible [0.55 μm] [*Hess et al.*, 1998]. *Satheesh et al.* [2006b] used aerosol measurements from shipborne and island platforms (for 8 years) to portray a comprehensive characterization of the spatial and temporal variation of radiative properties of aerosols over the Arabian Sea. They reported that average SSA (at 500 nm; measurement-based and column) over the northern Arabian Sea is 0.97 ± 0.03 during November to March and 0.93 ± 0.02 during the rest of the year. Measurement of SSA in UV spectral region is unavailable over the regions considered and hence it was not possible to make direct comparison, except a few in the past

Table 1. SSA and Aerosol Layer Height

	Atlantic: East		Atlantic: West		Arabian Sea	
Months in 2006	ω_0[a]	H (km)	ω_0	H (km)	ω_0	H (km)
Jan	0.859	2.59	0.893	2.78	0.918	2.89
Feb	0.869	2.76	0.878	2.90	0.921	3.18
Mar	0.907	3.01	0.916	2.95	0.930	3.82
Apr	0.881	2.73	0.906	2.93	0.943	3.54
May	0.861	2.77	0.896	3.06	0.932	4.11
Jun	0.877	2.85	0.898	3.40	0.904	4.51
Jul	0.875	3.08	0.893	3.40	0.893	4.29
Aug	0.874	3.08	0.887	3.77	0.897	4.08
Sep	0.868	2.69	0.886	2.94	0.931	4.22
Oct	0.886	3.07	0.909	3.27	0.936	3.32
Nov	0.883	3.37	0.898	4.07	0.942	3.19
Dec	0.876	2.93	0.893	3.08	0.887	3.17
Annual mean	0.876 ± 0.01	2.91 ± 0.22	0.896 ± 0.01	3.21 ± 0.39	0.920 ± 0.02	3.69 ± 0.54

[a]At 0.38 μm.

using TOMS and AERONET data simultaneous with models [*Colarco et al.*, 2002; *Sinyuk et al.*, 2003 are examples].

8. Summary and Conclusions

[42] The A-train is a constellation of six satellites, which provides an excellent opportunity to combine the strengths of different sensors and improve the accuracy of aerosol remote sensing [*Anderson et al.*, 2005]. The OMI operational aerosol retrieval is sensitive to aerosol optical depth, absorption and layer height. While MODIS aerosol retrieval is independent of aerosol layer height and not sensitive to aerosol absorption, it is sensitive to spectral aerosol optical depth and particle size. By using the MODIS retrieval to constrain the AOD in the OMI retrieval, we can improve assessments of aerosol absorption and layer height from OMI. Here we have demonstrated an approach to predict UV optical depths provided necessary adjustments (or corrections) are made on the basis of the curvature of the MODIS spectral AODs through the visible and near-IR ranges, from comparison to AERONET spectra. The MODIS-predicted UV optical depths were used to constrain the OMI inversion and obtain information on aerosol height from OMI and hence most importantly, improve the accuracy of the aerosol absorption product.

[43] The major conclusions of the study are listed below.

[44] 1. Over the Atlantic, agreement between OMI-retrieved and MODIS-predicted AOD is reasonably good throughout the year, which implies that the aerosol height assumed in the OMI algorithm is probably correct.

[45] 2. Over the Arabian Sea, agreement is acceptable only during months when transport of dust from Arabia dominates the aerosol (April to July). During rest of the year, large differences were observed between OMI-standard and MODIS-predicted AOD, which suggests inappropriate aerosol layer heights implicit in the OMI retrievals and/or use of desert dust instead of the carbonaceous aerosol model.

[46] 3. Constraining the analysis only for cases with larger UVAI (>1.5), yielded excellent agreement over the Atlantic throughout the year while improving the agreement over the Arabian Sea only during April to July when aerosol is dominated with dust. During rest of the year, the differences broadened in cases corresponding to large UVAI.

[47] 4. Validation of the retrievals using airborne lidar measurements indicate that layer heights (and hence aerosol absorption in UV) obtained from the OMI-MODIS combined retrieval are much closer to reality than the OMI-standard retrieval, in the Arabian Sea during March–May.

[48] 5. Uncertainty in the retrieval of UV absorption can be further reduced in the future with additional constrains in the assumptions in the OMI retrieval with particle size information from the MODIS retrieval.

[49] Measurements of ambient aerosol absorption in the UV spectral range are extremely rare, which make validation of the OMI absorption measurements impossible at this time. The UV spectral region is a particularly interesting spectral range to study and may hold information leading to speciation of aerosol particles from remote sensing.

[50] We have demonstrated the potential of multisatellite analysis of A-train data to improve the accuracy of retrieved aerosol products. Our analysis suggests that a combined OMI-MODIS-CALIPSO retrieval has great potential to further improve assessments of aerosol absorption. Significant advances in remote sensing of aerosol absorption will require continued development of reliable ground-based and airborne techniques that measure spectral absorption across the broad solar spectral range.

[51] **Acknowledgments.** This research was carried out when one of the authors (SKS) was supported by an appointment to the NASA postdoctoral program at the NASA Goddard Space Flight Center, administered by Oak Ridge Associated Universities through a contract with NASA. We also acknowledge funding through NASA's Atmospheric Composition program led by Phil DeCola and Rangasayi Halthore. We thank the principal investigators and their staff for establishing and maintaining the seven AERONET sites used in this investigation.

References

Anderson, T. L., et al. (2005), An "A-train" strategy for quantifying direct climate forcing by anthropogenic aerosols source, *Bull. Am. Meteorol. Soc.*, *86*, 1795–1808, doi:10.1175/BAMS-86-12-1795.

Andreae, M. O., C. D. Jones, and P. M. Cox (2005), Strong present-day aerosol cooling implies a hot future, *Nature*, *435*, 1187–1190, doi:10.1038/nature03671.

Arnott, W. P, et al. (2005), Towards aerosol light-absorption measurements with a 7-wavelength aethalometer: Evaluation with a photoacoustic instrument and 3-wavelength nephelometer, *Aerosol Sci. Technol.*, *39*(1), 17–29, doi:10.1080/027868290901972.

Asnani, G. C. (1993), *Tropical Meteorology*, vol. 1, 1012 pp., Indian Inst. of Tropical Meteorol., Pashan, Pune.

Bates, T. S. (1999), Preface, *J. Geophys. Res.*, *104*(D17), 21,645–21,647, doi:10.1029/1999JD900365.

Chin, M., R. B. Rood, S.-J. Lin, J.-F. Müller, and A. M. Thompson (2000), Atmospheric sulfur cycle simulated in the global model GOCART: Model description and global properties, *J. Geophys. Res.*, *105*(D20), 24,671–24,687, doi:10.1029/2000JD900384.

Colarco, P. R., O. B. Toon, O. Torres, and P. J. Rasch (2002), Determining the UV imaginary index of refraction of Saharan dust particles from Total Ozone Mapping Spectrometer data using a three dimensional model of dust transport, *J. Geophys. Res.*, *107*(D16), 4289, doi:10.1029/2001JD000903.

Diner, D. J., et al. (1998), Multi-angle Imaging SpectroRadiometer (MISR) description and experiment overview, *IEEE Trans. Geosci. Remote Sens.*, *36*(4), 1072–1087, doi:10.1109/36.700992.

Diner, D. J., J. C. Beckert, G. W. Bothwell, and J. I. Rodriguez (2002), Performance of the MISR instrument during its first 20 months in Earth orbit, *IEEE Trans. Geosci. Remote Sens.*, *40*(7), 1449–1466, doi:10.1109/TGRS.2002.801584.

Eck, T. F., B. N. Holben, J. S. Reid, O. Dubovik, A. Smirnov, N. T. O'Neill, I. Slutsker, and S. Kinne (1999), Wavelength dependence of the optical depth of biomass burning, urban, and desert dust aerosols, *J. Geophys. Res.*, *104*(D24), 31,333–31,349, doi:10.1029/1999JD900923.

Fraser, R. S., and Y. J. Kaufman (1985), The relative importance of aerosol scattering and absorption in remote sensing, *IEEE Trans. Geosci. Remote Sens.*, *GE-23*, 625–633, doi:10.1109/TGRS.1985.289380.

Hansen, J., M. Sato, and R. Ruedy (1997), Radiative forcing and climate response, *J. Geophys. Res.*, *102*(D6), 6831–6864, doi:10.1029/96JD03436.

Heintzenberg, J., et al. (1997), Measurements and modelling of aerosol single scattering albedo: Progress, problems, and prospects, *Beitr. Phys. Atmos.*, *70*(4), 249–263.

Hess, M., P. Koepke, and I. Schult (1998), Optical properties of aerosols and clouds: The software package OPAC, *Bull. Am. Meteorol. Soc.*, *79*, 831–844, doi:10.1175/1520-0477(1998)079<0831:OPOAAC>2.0.CO;2.

Holben, B. N., et al. (1998), AERONET: A federated instrument network and data archive for aerosol characterization, *Remote Sens. Environ.*, *66*, 1–16, doi:10.1016/S0034-4257(98)00031-5.

Horvath, H. (1993), Atmospheric light absorption: A review, *Atmos. Environ. Part A*, *27*(3), 293–317, doi:10.1016/0960-1686(93)90104-7.

Hsu, C., S. Tsay, M. D. King, and M. Herman (2004), Aerosol properties over bright-reflecting source regions, *IEEE Trans. Geosci. Remote Sens.*, *42*, 557–569.

Ichoku, C., D. A. Chu, S. Mattoo, Y. J. Kaufman, L. A. Remer, D. Tanré, I. Slutsker, and B. N. Holben (2002), A spatio-temporal approach for global validation and analysis of MODIS aerosol products, *Geophys. Res. Lett.*, *29*(12), 8006, doi:10.1029/2001GL013206.

Kaufman, Y. J., et al. (1998), Smoke, clouds, and radiation: Brazil (SCAR-B) experiment, *J. Geophys. Res.*, *103*(D24), 31,783–31,808, doi:10.1029/98JD02281.

Kaufman, Y. J., et al. (2001), Absorption of sunlight by dust as inferred from satellite and ground-based remote sensing, *Geophys. Res. Lett.*, *28*, 1479–1483, doi:10.1029/2000GL012647.

Kaufman, Y. J., D. Tanré, and O. Boucher (2002), A satellite view of aerosols in the climate system, *Nature*, *419*, 215–223, doi:10.1038/nature01091.

Kirchstetter, T. W, T. Novakov, and P. V. Hobbs (2004), Evidence that the spectral dependence of light absorption by aerosols is affected by organic carbon, *J. Geophys. Res.*, *109*, D21208, doi:10.1029/2004JD004999.

Levelt, P. F., et al. (2006), Ozone Monitoring Instrument, *IEEE Trans. Geosci. Remote Sens.*, *44*, 1093–1101, doi:10.1109/TGRS.2006.872333.

Levy, R. C., L. A. Remer, D. Tanré, Y. J. Kaufman, C. Ichoku, B. N. Holben, J. M. Livingston, P. B. Russell, and H. Maring (2003), Evaluation of the Moderate Resolution Imaging Spectroradiometer (MODIS) retrievals of dust aerosol over the ocean during PRIDE, *J. Geophys. Res.*, *108*(D19), 8594, doi:10.1029/2002JD002460.

Moorthy, K. K., S. K. Satheesh, S. S. Babu, and C. B. S. Dutt (2008), Integrated Campaign for Aerosols, Gases and Radiation Budget (ICARB): An overview, *J. Earth Syst. Sci.*, *117*, 243–262.

Ramanathan, V., et al. (2001), Indian Ocean Experiment: An integrated analysis of the climate forcing and effects of the great Indo-Asian haze, *J. Geophys. Res.*, *106*(D22), 28,371–28,398, doi:10.1029/2001JD900133.

Remer, L. A., et al. (2005), The MODIS aerosol algorithm, products, and validation, *J. Atmos. Sci.*, *62*, 947–973, doi:10.1175/JAS3385.1.

Russell, P. B., and J. Heintzenberg (2000), An overview of the ACE-2 clear sky column closure experiment (CLEARCOLUMN), *Tellus, Ser. B*, *52*(2), 463–483, doi:10.1034/j.1600-0889.2000.00013.x.

Satheesh, S. K., and K. K. Moorthy (2005), Radiative effects of natural aerosols: A review, *Atmos. Environ.*, *39*, 2089–2110, doi:10.1016/j.atmosenv.2004.12.029.

Satheesh, S. K., et al. (1999), A model for the natural and anthropogenic aerosols for the tropical Indian Ocean derived from Indian Ocean experiment data, *J. Geophys. Res.*, *104*(D22), 27,421–27,440, doi:10.1029/1999JD900478.

Satheesh, S. K., V. Vinoj, and K. K. Moorthy (2006a), Vertical distribution of aerosols over an urban continental site in India inferred using a micro pulse lidar, *Geophys. Res. Lett.*, *33*(20), L20816, doi:10.1029/2006GL027729.

Satheesh, S. K., K. K. Moorthy, Y. J. Kaufman, and T. Takemura (2006b), Aerosol optical depth, physical properties and radiative forcing over the Arabian Sea, *Meteorol. Atmos. Phys.*, *91*, 45–62, doi:10.1007/s00703-004-0097-4.

Schoeberl, M. R., et al. (2006), Overview of the EOS aura mission, *IEEE Trans. Geosci. Remote Sens.*, *44*, 1066–1074, doi:10.1109/TGRS.2005.861950.

Seinfeld, J. (2008), Atmospheric science: Black carbon and brown clouds, *Nature Geosci.*, *1*, 15–16, doi:10.1038/ngeo.2007.62.

Seinfeld, J. H., and S. N. Pandis (1998), *Atmospheric Chemistry and Physics: From Air Pollution to Climate Change*, 1326 pp., Wiley, New York.

Seinfeld, J. H., et al. (2004), ACE-ASIA: Regional climatic and atmospheric chemical effects of Asian dust and pollution, *Bull. Am. Meteorol. Soc.*, *85*, 367–380, doi:10.1175/BAMS-85-3-367.

Sinyuk, A, O. Torres, and O. Dubovik (2003), Imaginary refractive index of desert dust using satellite and surface observations, *Geophys. Res. Lett.*, *30*(2), 1081, doi:10.1029/2002GL016189.

Tanré, D., M. Herman, and Y. J. Kaufman (1996), Information on aerosol size distribution contained in solar reflected spectral radiances, *J. Geophys. Res.*, *101*(D14), 19,043–19,060, doi:10.1029/96JD00333.

Tanré, D., Y. J. Kaufman, M. Herman, and S. Mattoo (1997), Remote sensing of aerosol properties over oceans using the MODIS/EOS spectral radiances, *J. Geophys. Res.*, *102*(D14), 16,971–16,988, doi:10.1029/96JD03437.

Torres, O., P. K. Bhartia, J. R. Herman, and Z. Ahmad (1998), Derivation of aerosol properties from satellite measurements of backscattered ultraviolet radiation. Theoretical Basis, *J. Geophys. Res.*, *103*(D14), 17,099–17,110, doi:10.1029/98JD00900.

Torres, O., P. K. Bhartia, A. Sinyuk, E. J. Welton, and B. Holben (2005), Total Ozone Mapping Spectrometer measurements of aerosol absorption from space: Comparison to SAFARI 2000 ground-based observations, *J. Geophys. Res.*, *110*, D10S18, doi:10.1029/2004JD004611.

Torres, O., et al. (2007), Aerosols and surface UV products from Ozone Monitoring Instrument observations: An overview, *J. Geophys. Res.*, *112*, D24S47, doi:10.1029/2007JD008809.

Weingartner, E., et al. (2003), Absorption of light by soot particles: Determination of the absorption coefficient by means of aethalometers, *J. Aerosol Sci.*, *34*, 1445–1463, doi:10.1016/S0021-8502(03)00359-8.

T. F. Eck, B. N. Holben, R. G. Kleidman, and L. A. Remer, Laboratory for Atmospheres, NASA Goddard Space Flight Center, Greenbelt, MD 20771, USA.

S. K. Satheesh and V. Vinoj, Centre for Atmospheric and Oceanic Sciences, Indian Institute of Science, Bangalore 560012, India. (satheesh@caos.iisc.ernet.in)

S. S. Babu, Space Physics Laboratory, Vikram Sarabhai Space Centre, Thiruvananthapuram 695022, India.

O. Torres, Department of Atmospheric and Planetary Sciences, Hampton University, Hampton, VA 20668, USA.